Jurnal Teknologi

Full Paper

PREPARATION OF SPRAY DRIED COAMORPHOUS SOLIDS TO IMPROVE THE SOLUBILITY AND DISSOLUTION RATE OF ATORVASTATIN CALCIUM

Yudi Wicaksono[a*], Viddy Agustian Rosidi[a], Sri Yessika Saragih[a], Lyta Septi Fauziah[a], Dwi Setyawan[b]

[a]Drug Modification Research Group, Faculty of Pharmacy, University of Jember, Jember, 68121, Indonesia
[b]Faculty of Pharmacy, Airlangga University, Surabaya, 60286, Indonesia

Article history
Received
29 February 2020
Received in revised form
15 December 2020
Accepted
4 January 2021
Published online
23 February 2021

*Corresponding author
yudi.farmasi@unej.ac.id

Graphical abstract

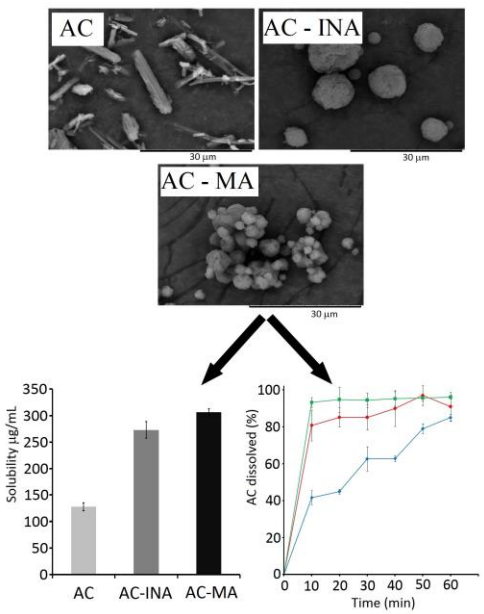

Abstract

Atorvastatin calcium (AC) is a statin drug used to lower cholesterol. Its crystalline form is usually found in the market with low solubility properties. The amorphization of crystalline AC is a technique used to increase its solubility however; the amorphous form has less thermodynamic stability. Therefore, to increase the solubility properties of its crystalline form, an AC coamorphous solid was prepared. This coamorphous solid was prepared using spray drying techniques, and coformers such as isonicotinamide (INA) and maleic acid (MA). Furthermore, characterization was carried out using powder X-ray diffraction, differential scanning calorimetry, fourier transform infrared spectroscopy, and scanning electron microscopy, while the solubility properties test was conducted using the shake-flask and paddle method. The results showed that the spray-dried solids were coamorphous with single-phase homogeneous systems. Furthermore, the coamorphous solids, AC-INA and AC-MA were found to have a higher Tg than the melting points of other components, and formed intermolecular interactions between them. The higher Tg and presence of intermolecular interactions indicate that coamorphous solids are more stable than the amorphous form. Therefore, the results of the solubility and dissolution test showed that the coamorphous solid of AC-INA and AC-MA have better solubility properties compared to the AC crystalline form.

Keywords: Coamorphous solid, atorvastatin, spray drying, solubility, intermolecular interaction

1.0 INTRODUCTION

Solubility and dissolution rates are parameters that determine the absorption of drugs in the gastrointestinal tract. This is because drugs need to dissolve in the gastrointestinal tract's biological fluids in order to be absorbed and provide their pharmacological effects [1]. Therefore, drugs with low solubility and dissolution rates usually experience oral bioavailability problems which pose challenges to pharmaceutical development [2, 3].

Atorvastatin calcium (AC) is a statin drug that is very potent in lowering blood cholesterol [4]. However, it has low water solubility (0.142 mg/ml) [5]. Research shows that a tablet of AC on the market has a solubility and dissolution efficiency of 55 and 46%, respectively [6, 7], therefore, these poor properties cause the drug's oral bioavailability to be only about 12% [5, 8, 9, 10]. This phenomenon occurs because the oral bioavailability of AC is limited by its solubility and dissolution rates [5].

One proven technique that increases the solubility and dissolution rate of AC is changing the

solid crystalline form to amorphous [5, 10, 11]. Amorphization increases the solubility and dissolution rates of crystalline solids because the molecules in the amorphous solid are weakly bound. Therefore, when dissolving amorphous solids, lower energy is required to break the cohesive interactions and dissolve molecules within the solvent [1, 12, 13]. The problem with these solids is that they often have low thermodynamic stability and a high tendency to revert to crystalline solids during storage or formulation process [14, 15]. However, this challenge can be solved through the formation of a coamorphous solid [14, 16], which are amorphous solids that consist of drugs and other small molecules called coformers [17, 18, 19]. Stability in coamorphous solid occurs through the formation of hydrogen bonds and π – π interactions between molecules of drugs and coformers that prevent molecular mobility, and the recrystallization of molecules [13, 14, 15].

Creating coamorphous solids in order to improve the solubility of AC can been carried out using the solvent evaporation and cooling method [20, 21]. However, there is a limitation to these methods, given that they are both difficult to make on a commercial scale [22, 23]. On the other hand, spray drying can be used to overcome problems related to upscaling [22]. When using this technique, intermolecular interactions are formed during the mixing of feed liquid and the spraying process which entails the rapid transfer of heat and mass. These processes form a coamorphous solid with optimal thermodynamic stability [22, 23]. Spray drying can catalyze the quick phase-change from liquid to solid, which increases the feasibility of upscaling [24]. Furthermore, this technique produces particles with good morphological properties so that they have excellent micromeritics characters [22]. Spray drying has already been used to form coamorphous solids from ibuprofen-arginine, budesonide-arginine, and indomethacin-lysin [23, 25, 26].

This study aims prepare a solid coamorphous form of AC that possesses higher solubility and dissolution rates than the crystalline form. The preparation of this solid was carried out using spray drying techniques with isonicotinamide (INA) and maleic acid (MA) as coformers. Both materials do not pose significant health risks when used with active pharmaceutical ingredients and in small quantities [27, 28]. Methanol was used to prepare the feed solution of the spray drying process because it dissolves AC and coformers (INA and MA) quite well. Furthermore, the use of methanol as a solvent in the formation of active coamorphous pharmaceutical compounds has been stated in several literature [10, 20, 29, 30].

2.0 METHODOLOGY

2.1 Materials

Pharmaceutical grade AC (98%) was provided as a gift sample by PT Dexa Medica (Palembang, Indonesia). While analytical grade INA (99%), MA (99%), and methanol (99.8%) were purchased from Sigma-Aldrich (Missouri, USA), Merck (Darmstadt, Germany), and Smart Lab (Tangerang, Indonesia) respectively.

2.2 Methods

2.2.1 Preparation of Coamorphous Solid

The AC and coformers (in equimolar ratios) were dissolved in methanol to obtain a feed solution with a concentration of 5% (w/v). This solution was spray-dried with an inlet and outlet temperature of 60 °C and 55 °C respectively. Furthermore, the feed rate was maintained at 5 mL/min with an air flow rate of 600 L/h and a pump rate of 5 ± 0.2 mL/min.

2.2.2 Solid State Characterization

Powder X-Ray Diffraction (PXRD)

The PXRD patterns were collected in a powder X-ray diffractometer (Philip Xpert) that made use of a Cu*Ka* radiation source (1.54060 Å), a voltage of 40 kV, and a current of 30 mA. The analysis was then carried out between 5 and 50° (2*θ*) with a scanning rate of 10°/min and a step size of 0.008°. Also, the divergence and anti-scattering slit were 0.25°.

Differential Scanning Calorimetry (DSC)

In this method, DSC thermograms were determined using a differential scanning calorimeter (Rigaku DSC 8230). Furthermore, calibration of the DSC's temperature and heat flow was carried out using high purity indium as a standard. 2.0 mg of the samples were accurately weighed in hermetic aluminum pans and then sealed. The DSC measurements were conducted at a rate of 10°C/min within the range of 30 – 250°C under a dry air atmosphere.

Fourier Transform Infrared Spectroscopy (FTIR)

The FTIR analysis of samples was recorded using a fourier transform infrared spectrophotometer (Bruker Alpha FTIR spectrometer) equipped with an attenuated total reflectance. Consequently, the measurements were performed at a resolution of 4 $cm^{-1}$and in the range of 4000-600 cm^{-1}.

Scanning Electronic Microscopy (SEM)

The morphology of the spray-dried solid was examined using a scanning electron microscope (Hitachi TM-3000). Subsequently, a double-sided carbon tape was placed on a stainless steel stub and the samples were spread over the tape. Any excess powder was removed using pressurized air, and the samples on the stub were then coated with platinum using a sputter coater ion (Hitachi E-1045) at 40 mA for 20 seconds. All SEM images were analyzed at 15 kV accelerating voltage which is appropriate for magnification.

2.2.3 Solubility Studies

The saturation solubility test was conducted using the shake-flask method. An additional amount of sample powder was added to 25 ml of distilled water contained in a 100-mL Erlenmeyer flask. The resultant suspensions were shaken in an orbital shaker at a temperature of 37 °C and constantly stirred at 150 rpm for 12 hours. The solutions containing samples were collected and filtered through a 0.45 µm membrane filter, after which the clear supernatant was diluted and a UV-Vis spectrophotometer was used to estimate their concentrations. Testing was performed with three repetitions.

2.2.4 In Vitro Dissolution Testing

The dissolution test was carried out by the paddle method using a dissolution tester (Logan UDT-804) at 100 rpm and 37 ± 0.5 °C. The samples (equivalent to 20 mg of AC) were introduced to 900 mL of distilled water within the chamber. Consequently, at each time interval (10, 20, 30, 40, 50, and 60 min), 5 mL of the eluted sample was withdrawn from the chamber and replaced with an equal amount of distilled water. The samples were filtered through a 0.45 µm membrane filter, and the AC concentration was analyzed using a UV-Vis spectrophotometer. Testing was also performed with three repetitions.

3.0 RESULTS AND DISCUSSION

3.1 PXRD Diffractogram

PXRD analysis is used to determine the physical phase of solid materials. Therefore, the formation of the amorphous phase was confirmed when a halo pattern appeared as a curve without crystalline peaks on the diffractogram [16]. The PXRD patterns of crystalline AC, AC-INA, and AC-MA are shown in Figure 1. That of crystalline AC shows sharp diffraction peaks of 2θ at 9.4, 10.2, 11.8, 17.0, 19.4, 21.6, and 23.7°. This indicates the presence of a crystalline solid, which agrees with previous reports [11, 31]. The PXRD patterns of AC-INA and AC-MA indicated the absence of sharp diffraction peaks and the presence of typical halo patterns, which suggest amorphicity [21]. These results show that spray dried solids of AC with INA and MA coformers forms a coamorphous solid system [19, 20, 31].

3.2 DSC Thermogram

DSC is a technique used to analyze thermal events related to the phase transitions of solid materials [18, 32]. Therefore, the phase transitions obtained from DSC thermograms can be used to strengthen the alleged amorphicity [21]. DSC can also be used to estimate the phase solubility of amorphous materials. When applied to the single-phase homogeneous systems of amorphous materials, DSC thermograms can be used to track changes from its glass to a viscous state [13]. The DSC thermogram of crystalline AC, AC-INA, and AC-MA are shown in Figure 2. That of crystalline AC shows a sharp endothermic peak at 155.0 °C (ΔH= 69 J/g) corresponding with the melting point of the material. This result agrees with previously reported values [5]. Meanwhile, the DSC thermograms of AC-INA and AC-MA showed a single Tg at 209.1 and 182.0 °C, respectively, which confirms the amorphicity of a new co-amorphous system phase [19, 33]. The Tg of co-amorphous AC-INA and AC-MA showed higher temperatures than the melting point of crystalline AC. Therefore, the relatively higher Tg of the coamorphous system indicates that intermolecular interactions such as hydrogen bonding between functional groups of drug and coformers were occurring [21]. In general, the intermolecular interactions within the coamorphous system increase its stability and reduces crystallization tendency [13].

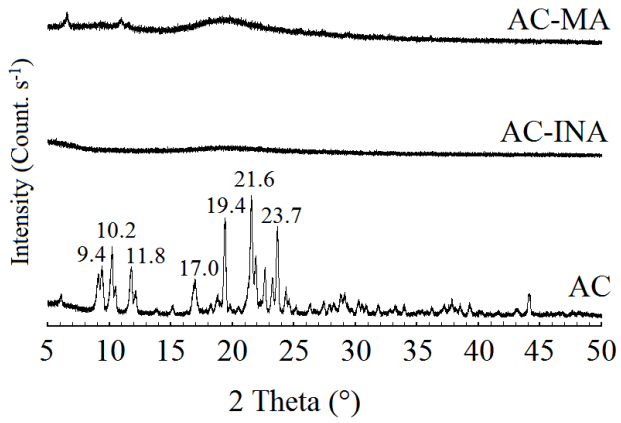

Figure 1 PXRD diffractograms of AC, AC-INA, and AC-MA

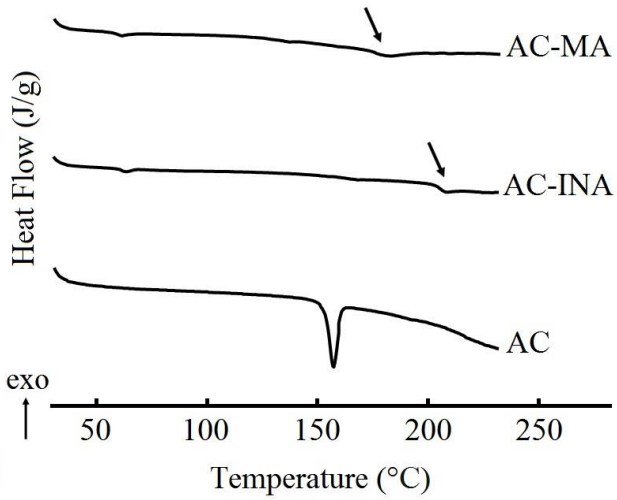

Figure 2 DSC thermograms of AC, AC-INA, and AC-MA

The ability of the coamorphous system to mix easily is a strong determiner of glass stability [18]. In addition, the single Tg value of AC-INA and AC-MA indicates that the components in the coamorphous systems were miscible with each other through the formation of a single-phase homogeneous system [13, 34]. Thus the

coamorphous AC-INA and AC-MA can be expected to increase the physical stability of amorphous systems.

Based on the results of DSC characterization, coamorphous solid thermograms of AC-INA and AC-MA showed a small endothermic peak at 70 °C, indicating the loss of methanol residue from samples [35]. Therefore, if this method is used to prepare coamorphous solids of AC-INA and AC-MA (ready to use by consumers), the removal of residual methanol will need to be perfected.

3.3 FTIR Spektra

FTIR spectroscopy analysis can be used to investigate the possible molecular interactions between AC, INA, and MA in coamorphous systems. The presence of non-covalent interactions such as hydrogen and π-π bonding can be identified in the FTIR spectra through shifts or the broadening of absorption peaks in the functional groups of the components [16, 33, 36]. For crystalline AC, the absorption peaks of the functional groups can be seen at 3364 cm-1 (free NH stretching), 3056 cm-1 (OH stretching), 1650 cm-1 (C = O stretching), and 1216 cm-1 (CN stretching) (Figure 3). Consequently, the position of crystalline AC absorption peaks agrees with previous reports [10, 31].

The FTIR spectra of coamorphous AC-INA and AC-MA (Figure 3) showed broad peaks and reduced intensity when compared to that of crystalline AC (Figure 3). This broadening and reduction were attributed to amorphization caused by the disruption of the crystal lattice and the lack of long-range orders for a specific bond [17, 19, 37]. Furthermore, the absorption peaks of coamorphous AC-INA exhibited shifts from lower to higher wave numbers (3364 to 3415 cm-1, 3056 to 3069 cm-1, 1650 to 1664 cm-1, and 1216 to 1223 cm-1). There were also shifts in the absorption peaks at 3364 to 3402 cm-1, 3056 to 3063 cm-1, 1650 to 1661 cm-1, and 1216 to 1223 cm-1.

All these shifts particularly in AC indicate the formation of intermolecular interactions between the functional group components [37]. The functional groups of AC which form intermolecular interactions with coamorphous AC-INA and AC-MA are strong proton acceptors and donors of hydrogen bond, therefore hydrogen bonding is present [22, 38]. This indicates that the coamorphous solid systems of AC-INA and AC-MA are in single miscible phases [33].

3.4 Morphology

A scanning electron microscope was used to observe the morphological characteristics of the crystalline and coamorphous AC. The microphotograph of crystalline AC, coamorphous AC-INA, and AC-MA are presented in Figure 4. The crystalline AC exhibited the formation of long, needle-shaped crystals of different sizes. Microphotographs of coamorphous AC-INA and AC-MA showed a round-shaped morphology with a porous surface attributed to the presence of amorphous solids. The structure of coamorphous AC-MA was much smaller than that of coamorphous AC-INA. These substances exhibited microstructures devoid of needle-shaped AC crystals and coformers during the spray drying process, resulting in the instantaneous formation of coamorphous solid [22].

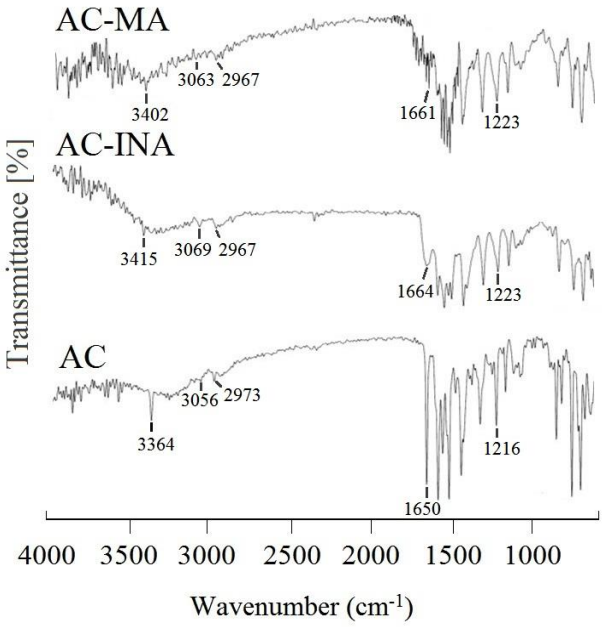

Figure 3 FTIR spectra of AC, AC-INA, and AC-MA

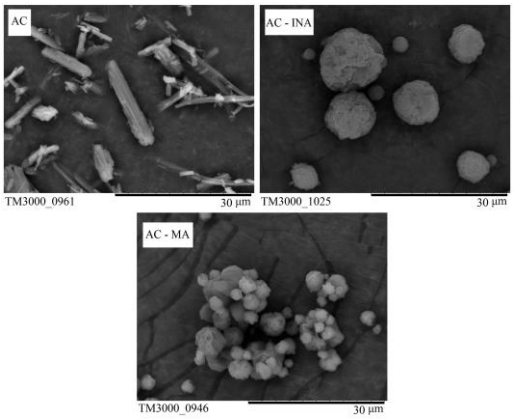

Figure 4 SEM Images of AC, AC-INA, and AC-MA

3.5 Solubility

Solubility is an important factor in bioavailability and therapeutic efficacy of drugs that are poorly water-soluble. Therefore, the formation of coamorphous systems has been hypothesized to be one of the most effective strategies for improving the solubility of poorly water-soluble drugs, thereby increasing their bioavailability [18]. The solubility of crystalline AC, coamorphous AC-INA and AC-MA in water was 127.63, 272.94, and 306.71 µg / mL, respectively (Figure 5). The solubility of coamorphous AC-INA and AC-MA were found to be significantly higher than that of crystalline AC. After enhancement, the solubility of AC-INA and

AC-MA was found to be 2.0 and 2.5 fold more than of AC.

In thermodynamics, solubility depends on a balance between two kinds of interactions. The first being how tight the molecules are bound to their solid state and the second, how strongly these molecules associate with the solvent [39]. A solid being freely soluble in a solvent indicates that the molecules are weakly bound in the solid state. When dissolving a soluble solid, lower energy is needed to break the cohesive interactions between molecules which allow it to dissolve in the solvent [13]. The coamorphous AC-INA and AC-MA had increased solubility due to the low energy needed to breaking the cohesive interactions between the molecules [13]. In addition, the larger surface area and porous nature of AC-INA and AC-MA's coamorphous systems might have played a role in their increase in solubility [22, 40].

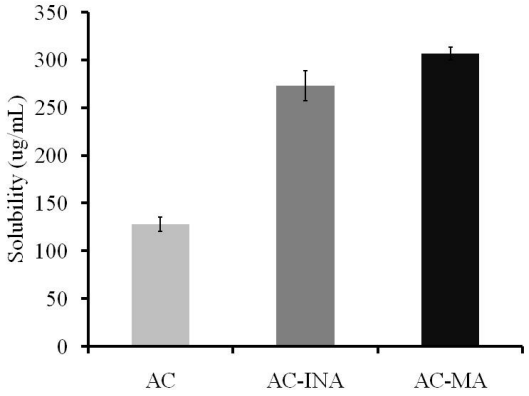

Figure 5 Solubility of AC, AC-INA, and AC-MA

3.6 Dissolution Behavior

The dissolution profile of crystalline AC, coamorphous AC-INA, and AC-MA are shown in Figure 6. AC-INA and AC-MA exhibited faster dissolution rates when compared with crystalline AC. The amount of AC crystals that dissolved under 10 and 30 minutes were 42% and 63% respectively. Furthermore, the amount of coamorphous AC-INA and AC-MA that dissolved under 10 minutes was 80% and 93%, while 30 minutes yielded 85% and 94 %, respectively. From the dissolution test (10 min), coamorphous solids of AC-INA and AC-MA showed a 1.94 and 2.24 fold enhancement when compared to AC. These results suggest that the coamorphous solid of AC-INA and AC-MA showed significant improvement in dissolution behavior when compared to crystalline AC. In addition, coamorphous AC-MA displayed faster dissolution rates than coamorphous AC-INA. This result is thought to be because AC-MA's particles are smaller than that of AC-INA. The small particle size and larger surface area lead to an increase in the dissolution rate [40]. The higher solubility of coamorphous AC-MA compared to AC-INA might also contribute to the overall increases in its dissolution behavior [41].

The oral absorption and bioavailability of a drug are largely determined by its solubility and dissolution rate. Therefore, the oral bioavailability of poorly water-soluble drugs can be improved by increasing their solubility and dissolution rates [5,40]. The results of the dissolution test showed that the spray-dried coamorphious solid of AC-INA and AC-MA had better dissolution behaviors when compared to AC's crystalline form. Therefore, these results suggest that the coamorphous AC-INA and AC-MA may increase the oral bioavailability of AC.

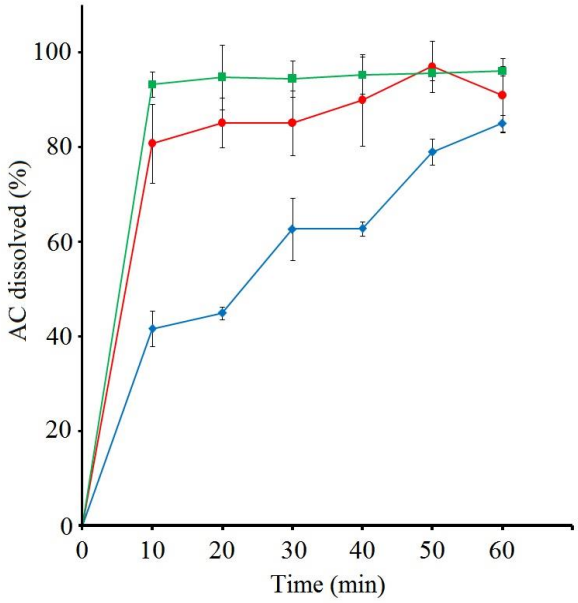

Figure 6 Dissolution profiles of crystalline AC (blue line), co-amorphous AC-INA (red line), and co-amorphous AC-MA (green line)

4.0 CONCLUSION

The coamorphous solid of AC-INA and AC-MA were successfully prepared using spray drying techniques. Within the coamorphous systems, the AC and coformers formed intermolecular interactions, which made it more stable than the conventional amorphous form. Compared to crystalline AC, the solubility of AC-INA and AC-MA (coamorphous solid) in water recorded significant improvement. The dissolution test carried out in water proved that the coamorphous solid of AC-INA and AC-MA has greater dissolution behavior compared to AC crystalline form. In conclusion, the formation of coamorphous solids through spray drying techniques is an effective technique for improving the solubility and dissolution behavior of AC crystalline form.

Acknowledgement

The authors would like to thank Rector of University of Jember for the research funding through IDB Project grant 2019 (Hibah Mendukung Program IDB) decree number 13455/UN25/LT/2019 under contract number 3246/UN25.3.1/LT/2019.

References

[1] Williams, R. O., A. B. Watts, and D. A. Miller. 2016. *Formulating Poorly Water Soluble Drugs*. Cham: Springer Nature.

[2] *Kawabata Y,* Wada K, Nakatani M, Yamada S, and Onoue S. 2011. Formulation Design for Poorly Water-Soluble Drugs Based on Biopharmaceutics Classification System: Basic Approaches and Practical Applications. *International Journal of Pharmaceutics*. 420: 1-10.

[3] Athiyah, U., P. A. Kusuma, Tutik, M. L. A. D. Lestari, D. Isadiartuti, D. P. Paramita, and D. Setyawan. 2019. Crystal Engineering of Quercetin by Liquid Assisted Grinding Method. *Jurnal Teknologi*. 81(1): 39-45. DOI: https://doi.org/10.11113/jt.v81.12639.

[4] Yassine, H. 2015. *Lipid Management*. Cham: Springer Science.

[5] *Kim,* J. S., M. S. *Kim,* H. J. Park, S. J. Ji, S. Lee, and S. J. Hwang. 2008. Physicochemical properties and oral bioavailability of amorphous atorvastatin hemi-calcium using spray-drying and SAS process. *International Journal of Pharmaceutics*. 359: 211-219. DOI: https://doi:10.1016/j.ijpharm.2008.04.006

[6] Khan, F. N., and M. H. G. Dehghan. 2012. Enhanced Bioavailability and Dissolution of Atorvastatin Calcium from Floating Microcapsules Using Minimum Additives. *Scientia Pharmaceutica*. 80(1): 215-28. DOI : http://dx.doi.org/10.3797/scipharm.1104-26

[7] Oishi, T. S., I. Nimmi, and S. M. A. Islam. 2011. Comparative *in vitro* Bioequivalence Analysis of Some Generic Tablets of Atorvastatin, a BCS Class II Compound. *Bangladesh Pharmaceutical Journal.* 14(1): 61-66.

[8] Shaker, A. M. 2018. Dissolution and Bioavailability Enhancement of Atorvastatin: Gelucire Semisolid Binary System. *Journal of Drug Delivery Science and Technology*. 43: 178-184. DOI: http://dx.doi.org/10.1016/j.jddst.2017.10.003.

[9] Rodde, M. S., G. T. Divase, T. B. Devkar, and A. R. Tekade. 2014. Solubility and Bioavailability Enhancement of Poorly Aqueous Soluble Atorvastatin: *In Vitro*, *Ex Vivo*, and *In Vivo* Studies. *BioMed Research International*. 2014: 463895. DOI: http://dx.doi.org/10.1155/2014/463895.

[10] *Kim, M. S.,* S. J. Jin, J. S. *Kim,* H. J. Park, H. S. Song, R. H.H. Neubert, and S. J. Hwang. 2008. Preparation, Characterization and In Vivo Evaluation of Amorphous Atorvastatin Calcium Nanoparticles Using Supercritical Antisolvent (SAS) Process. *International Journal of Pharmaceutics*. 69: 454-465. DOI: https://doi:10.1016/j.ejpb.2008.01.007.

[11] Choudhary, A., A. C. Rana, G. Aggarwal, V. Kumar, and F. Zakir. 2012. Development and Characterization of an Atorvastatin Solid Dispersion Formulation Using Skimmed Milk for Improved Oral Bioavailability. *Acta Pharmaceutica Sinica B*. 2(4): 421-428. DOI: http://dx.doi.org/10.1016/j.apsb.2012.05.002.

[12] Dhokchawle B. V., S. J. Tauro, and A. B. Bhandari. 2013. Amorphous Pharmaceutical Solids: A Review. *Indian Drugs*. 50(07): 5-13.

[13] Karagianni, A., K. Kachrimanis, and I. Nikolakakis. 2018. Co-Amorphous Solid Dispersions for Solubility and Absorption Improvement of Drugs: Composition, Preparation, Characterization and Formulations for Oral Delivery. *Pharmaceutics*. 10(3): 98. DOI: http://dx.doi.org/10.3390/pharmaceutics10030098.

[14] Laitinen, R., K. Löbmann, C. J. Strachan, H. Grohganz, and T. Rades. 2013. Emerging Trends in the Stabilization of Amorphous Drugs. *International Journal of Pharmaceutics*. 453: 65-79. DOI: http://dx.doi.org/10.1016/j.ijpharm.2012.04.066.

[15] Vo, C. L. N., C. Park, and B. J. Lee. 2013. Current Trends and Future Perspectives of Solid Dispersions Containing Poorly Water-soluble Drugs. *European Journal of Pharmaceutics and Biopharmaceutics*. 85: 799-813. DOI: http://dx.doi.org/10.1016/j.ejpb.2013.09.007.

[16] Chavan, R. B., R. Thipparaboina, D. Kumar, and N. R. Shastri. 2016. Co Amorphous Systems: A Product Development Perspective. *International Journal of Pharmaceutics*. 515: 403-415. DOI: http://dx.doi.org/10.1016/j.ijpharm.2016.10.043.

[17] Ueda, H., N. Muranushi, S. Sakuma, Y. Ida, T. Endoh, K. Kadota, and Y. Tozuka. 2016. A Strategy for Co-former Selection to Design Stable Co-amorphous Formations Based on Physicochemical Properties of Non-steroidal Inflammatory Drugs. *Pharmaceutical Research*. 33: 1018-1029. DOI: http://dx.doi.org/10.1007/s11095-015-1848-2.

[18] Shi, Q., S. M. Moinuddin, T. Cai. 2019. Advances in Coamorphous Drug Delivery Systems. *Acta Pharmaceutica Sinica B*. 9(1): 19-35. DOI: https://dx.doi.org/10.1016/j.apsb.2018.08.002.

[19] Wang, J., R. Chang, Y. Zhao, J. Zhang, T. Zhang, Q. Fu, C. Chang, and A. Zeng. 2017. Coamorphous Loratadine-Citric Acid System with Enhanced Physical Stability and Bioavailability. *AAPS PharmSciTech*. 18(7): 2541-2550. DOI: http://dx.doi.org/10.1208/s12249-017-0734-0.

[20] Shayanfar, A., H. Ghavimi, H. Hamishehkar, and A. Jouyban. 2013. Coamorphous Atorvastatin Calcium to Improve its Physicochemical and Pharmacokinetic Properties. *Journal of Pharmmacy and Pharmaceutical Sciences*. 16(4): 577-587.

[21] Nair, A., R. Varma, K. Gourishetti, K. Bhat, and S. Dengale. 2019. Influence of Preparation Methods on Physicochemical and Pharmacokinetic Properties of Co-amorphous Formulations: The Case of Co-amorphous Atorvastatin: Naringin. *Journal of Pharmaceutical Innovation*. DOI: https://dx.doi.org/10.1007/s12247-019-09381-9.

[22] Wairkar, S., and R. Gaud. 2019. Development and Characterization of Microstructured, Spray-Dried Co-Amorphous Mixture of Antidiabetic Agents Stabilized by Silicate. *AAPS PharmSciTech*. 20: 141. DOI: https://dx.doi.org/10.1208/s12249-019-1352-9.

[23] Kasten, G., Í. Duarte, M. Paisana, K. Löbmann, T. Rades, and H. Grohganz. 2019. Process Optimization and Upscaling of Spray-Dried Drug-Amino acid Co-Amorphous Formulations. *Pharmaceutics*. 11(1): 24. DOI: https://dx.doi.org/10.3390/pharmaceutics11010024

[24] Bello, A. A., A. Ahmad, A. Ripin, and O. Oladokun. 2016. Numerical Estimation of Moisture Content in Spray Dried Juice Powder. *Jurnal Teknologi*. 78(8-3): 65-70.

[25] Ojarinta, R., L. Lerminiaux, and R. Laitinen. Spray Drying of Poorly Soluble Drugs from Aqueous Arginine Solution. *International Journal of Pharmaceutics*. 532(1): 289-298. DOI: https://dx.doi.org/10.1016/j.ijpharm.2017.09.015.

[26] Lu, W., T. Rades, J. Rantanen, and M. Yang. 2019. Inhalable Co-amorphous Budesonide-arginine Dry Powders Prepared by Spray Drying. *International Journal of Pharmaceutics*. 565: 1-8. DOI: https://dx.doi.org/10.1016/j.ijpharm.2019.04.036.

[27] Bhalla, Y., K. Chadha, R. Chadha, and M. Karan. 2019. Daidzein cocrystals: An Opportunity to Improve Its Biopharmaceutical Parameters. *Heliyon*. 5(11): e02669. DOI: https://dx.doi.org/10.1016/j.heliyon.2019.e02669.

[28] Han, Y., Y. Pan., Lv, J., Guo, W., and Wang, J. 2016. Powder Grinding Preparation of Co-Amorphous B-Azelnidipine and Maleic Acid Combination: Molecular Interactions and Physicochemical Properties. *Powder Technology*. 291: 110-120. DOI: https://dx.doi.org/10.1016/j.powtec.2015.11.068.

[29] Zhang, H., X., J. X. Wang, Z. B. Zhang, Y. Le, Z. G. Shen, and J. F. Chen. 2009. Micronization of Atorvastatin Calcium by Antisolvent Precipitation Process. *International Journal of Pharmaceutics*. 374(1-2): 106-113. DOI: https://doi.org/10.1016/j.ijpharm.2009.02.015.

[30] Ainurofiq, A., R. Mauludin, D. Mudhakir, and S. N. Soewandhi. 2018. A Novel Desloratadine-Benzoic Acid Co-Amorphous Solid: Preparation, Characterization, and Stability Evaluation. *Pharmaceutics*. 10(3): 85. DOI: https://dx.doi.org/10.3390/pharmaceutics10030085

[31] Wicaksono, Y., D. Setyawan, Siswandono, and T. A. Siswoyo. 2019. Preparation and Characterization of a Novel Cocrystal of Atorvastatin Calcium with Succinic

Acid Coformer. *Indonesian Journal of Chemistry*. 19(3): 660-667.
DOI: https://dx.doi.org/10.22146/ijc.35801

[32] Wicaksono, Y., D. Setyawan, and S. Siswandono. 2018. Multicomponent Crystallization of Ketoprofen-nicotinamide for Improving the Solubility and Dissolution Rate. *Chemistry Journal of Moldova*. 13(2): 74-81.
DOI: http://dx.doi.org/10.19261/cjm.2018.493.

[33] Angeles, J. C., M. Videa, and L. M. Martínez. 2019. Highly Soluble Glimepiride and Irbesartan Co-amorphous Formulation with Potential Application in Combination Therapy. *AAPS PharmSciTech*. 20(4): 144.
DOI: https://dx.doi.org/10.1208/s12249-019-1359-2.

[34] Newman, A., S. M. R. Edens, and G. Zografi. 2018. Coamorphous Active Pharmaceutical IngredienteSmall Molecule Mixtures: Considerations in the Choice of Coformers for Enhancing Dissolution and Oral Bioavailability. *Journal of Pharmaceutical Sciences*. 107(1): 5-17.
DOI: https://dx.doi.org/10.1016/j.xphs.2017.09.024.

[35] Chadha, R., A. Kuhad, P. Arora, and S. Kishor. 2012. Characterisation and Evaluation of Pharmaceutical Solvates of Atorvastatin Calcium by Thermoanalytical and Spectroscopic Studies. *Chemistry Central Journal*. 6(1): 114-129.
DOI: https://doi.org/10.1186/1752-153X-6-114.

[36] Jiménez, C. M., J. C. Angeles, M. Videa, and L. M. Martínez. 2018. Co-Amorphous Simvastatin-Nifedipine with Enhanced Solubility for Possible Use in Combination Therapy of Hypertension and Hypercholesterolemia. *Molecules*. 23(9): 2161.
DOI: https://dx.doi.org/10.3390/molecules23092161.

[37] D'Angelo, A., B. Edgar, A. P. Hurt, and M. D. Antonijevic. 2018. Physico-chemical Characterisation of Three-Component Co-Amorphous Systems Generated by a Melt-Quench Method. *Journal of Thermal Analysis and Calorimetry*. 134: 381-390.
DOI: https://dx.doi.org/10.1007/s10973-018-7291-y.

[38] Wairkar, S., and R. Gaud. 2016. Co-Amorphous Combination of Nateglinide-Metformin Hydrochloride for Dissolution Enhancement. *AAPS PharmSciTech*. 17(3): 673-681.
DOI: https://dx.doi.org/10.1208/s12249-015-0371-4.

[39] Kuleshova, L. N., D. W. M. Hofmann, and R. Boese. 2013. Lattice Energy Calculation – A Quick Tool for Screening of Cocrystals and Estimation of Relative Solubility. Case of Flavonoids. *Chemical Physics Letters*. 564: 26-32.
DOI: https://doi.org/10.1016/j.cplett.2013.02.008.

[40] Khadka, P., J. Ro, H. Kim, I. Kim, J. T. Kim, H. Kim, J. M. Cho, G. Yun, and J. Lee. 2014. Pharmaceutical Particle Technologies: An Approach to Improve Drug Solubility, Dissolution and Bioavailability. *Asian Journal of Pharmaceutical Sciences*. 9(6): 304-316

[41] Sterren, V. B., V. Aiassa, C. Garnero, Y. G. Linck, A. K. Chattah, G. A. Monti, M. R. Longhi, and A. Zoppi. 2017. Preparation of Chloramphenicol/Amino Acid Combinations Exhibiting Enhanced Dissolution Rates and Reduced Drug-Induced Oxidative Stress. *AAPS PharmSciTech*. 18(8): 2910-2918.
DOI: https://dx.doi.org/10.1208/s12249-017-0775-4.